Available online at www.sciencedirect.com
ScienceDirect
International Journal of Mass Spectrometry 264 (2007) 61–69
International Journal of Mass Spectrometry
www.elsevier.com/locate/ijms

# Gas-phase positive and negative ion/molecule reactions in diborane and silane/diborane mixtures

Lorenza Operti, Roberto Rabezzana*, Francesca Turco, Gian Angelo Vaglio

*Dipartimento di Chimica Generale ed Organica Applicata and NIS Centre of Excellence, Università degli Studi di Torino, Corso Massimo d'Azeglio 48, Turin 10125, Italy*

Received 27 February 2007; received in revised form 23 March 2007; accepted 26 March 2007
Available online 4 April 2007

**Abstract**

The gas phase ion chemistry of diborane and of silane/diborane mixtures was studied by ion trap mass spectrometry (ITMS), in both positive and negative ionization mode. Positive ion/molecule reactions in diborane mainly proceed through $H_2$ or $BH_3$ loss and lead to formation of B hydride clusters containing up to six B atoms, while in negative ionization clustering reactions proceed to a higher degree with formation of $B_8H_n^-$ ions. In the silane/diborane system, the main ion/molecule reactions leading to ions containing both silicon and boron atoms were identified and rate constants of the main processes were determined for positive ions. In positive ionization, Si/B ions are mainly formed in reactions of few diborane ions with silane, while reactions of silane ions with $B_2H_6$ yield $B_2H_5^+$ as the main product. Negative ionization of the same mixture produces a much larger amount of Si/B ionic species, due to several reactions of silane anions with diborane, resulting in $BH_3$ or $H_2$ neutral losses. These results indicate that negative ions may play an important role in formation of Si/B ion clusters in plasma chemical vapour deposition processes for production of semiconductor and photovoltaic materials.


*Keywords:* Gas-phase ion chemistry; Ion trap mass spectrometry; Silane; Diborane; Negative ion

## 1. Introduction

Boron ions implantation in silicon substrates is a well-known method for manufacturing integrated circuits [1], and the first patents regarding this technology date back to the early 1980s [2,3]. Despite its many advantages, ion implantation displays some negative features such as high costs and necessity of annealing for activation of the material. Chemical vapour deposition (CVD) from appropriate gas mixtures represents an option in order to obtain amorphous or crystalline silicon thin films which may be employed for solar cells [4,5] or field effect transistors [6–8]. In particular, CVD and plasma-enhanced CVD (PE-CVD) of appropriate mixtures of silane and boron-containing molecules allows to obtain Si materials p-doped by boron atoms without any further treatment [9,10]. However, the chemical reactions occurring in the first steps of the processes, which involve radicals, neutrals and ion species, are still largely unknown. Ion reactions are particularly relevant in the ionization CVD process [11], where it is proved that ionization of source gases reduces Brownian coagulation of the nanoparticles formed in the CVD reactor. Recently, Hu et al. studied the gas phase reactions of neutral species in $SiH_4$–$BH_3$ [12] and $SiH_4$–$B_2H_6$ [13] mixtures by high-level ab initio calculations. Early studies of positive and negative ion/molecule chemistry of diborane were reported by Dunbar [14], who also studied the higher homologues $B_4$–$B_6$ [15] and positive ion/molecule reactions of diborane with oxygen-containing compounds [16]. More recently, experimental and theoretical studies of the reactions of $B_2H_3^-$ with carbon dioxide and sulfides were carried out [17,18], as well as of the $BH_2^+$ cation with several small molecules [19,20]. Further theoretical calculations concern a study of the $B_2H_5^+$, $B_2H_6^+$ and $B_2H_6$ species [21], the reaction of $B_2H_6$ with ammonia [22], and the determination of the proton affinity of diborane [23].

The gas-phase positive ion chemistry of silane has been extensively studied, both experimentally and theoretically [24–30]. As far as negative ions are concerned, ab initio calculations determined the structures and electron affinities of $Si_nH_m^-$

* Corresponding author. Tel.: +39 011 6707587; fax: +39 011 2367587.
*E-mail address:* roberto.rabezzana@unito.it (R. Rabezzana).

1387-3806/$ – see front matter © 2007 Elsevier B.V. All rights reserved.
doi:10.1016/j.ijms.2007.03.018

($n = 1$–3) anions [31,32], while anion/molecule reactions in silane were reported by Reents [33] and by our group [34]. In the present paper, ion/molecule reactions occurring in ionized silane/diborane mixtures are studied by ion trap mass spectrometry, with the aim to unravel the contribution of positive and negative ion species in the first nucleation processes occurring during CVD from $SiH_4$ and $B_2H_6$. From a fundamental point of view, the present work also aims to extend the knowledge of the intrinsic reactivity of ion species in the gas phase, where the solvent and counterions are absent.

## 2. Experimental

All the reagent gases were supplied by SIAD (Bergamo, Italy) in high purity (diborane has been provided diluted with $N_2$, in proportion of 1:4, for safety reasons). Helium buffer gas was supplied by SIAD at an extra-high purity grade and was used without further purification.

All the experiments in positive ionization mode were run on a Finnigan (Austin, TX, USA) ITMS instrument maintained at 333 K in order to obtain results comparable to those obtained from previous studies [34–37]. Pressures were measured by a Bayard Alpert ion gauge and corrected for both the relative sensitivity of the ion gauge with respect to different gases (M. Decouzon, J.-F. Gal, P.-C. Maria, A.S. Tchinianga, personal communication) and a calibration factor, which depends on the geometry of the instrument, experimentally determined as reported previously [30]. The manifold and the lines for introduction of gases were frequently baked out in order to avoid side reactions with water background. Total reagent gas pressures were typically $1.2 \times 10^{-6}$ Torr (1 Torr = 133.3 Pa), helium buffer gas pressure was $7.0 \times 10^{-5}$ Torr in all experiments. At this buffer gas pressure, empirically set in order to maximize the abundance of signals, it is reasonable to assume that most of the ions are kinetically thermalized. Ionization was achieved by electron ionization using an electron beam with an average energy of 35 eV. For diborane and silane/diborane systems three kinds of experiment were performed: (1) *Detection of all species without any ion isolation*: a suitable reaction time follows the ionization event in order to observe reaction between the ions and neutral substrates. Spectra are acquired at increasing reaction times (from 0 to 1 s) in order to follow variations of ion abundances with time. (2) *Detection of reaction paths*: ion species identified in previous experiments are isolated one by one and stored in the trap for increasing times (from 0 to 1 s) to identify their products generated by reactions with neutral molecules and to observe their trend with reaction time. Selective isolation of ions was achieved by the apex method (superimposition of dc and rf voltages). (3) *Kinetic rate constants measurement*: after isolation, ions were allowed to react for a shorter reaction time (from 0 to 40 ms) to avoid consecutive reactions of primary product ions. Spectra are recorded every 0.2 ms in order to get a relevant number of data for calculations. The procedures have been previously described in detail [30]. Experiments for the determination of each rate constant have been repeated two or three times and the results reported here are the means of the calculated values. In all experiments ions have been detected in the 10–300 u mass range.

The experiments in negative ionization mode were performed on a Finnigan GCQ Polaris mass spectrometer held at room temperature. Ions were formed with an electron beam at an average energy of 35 eV. Ionization time was 25 ms. Two different types of ion volumes (source geometry), i.e., one for electron ionization (EI) and one for chemical ionization (CI), were employed. The EI ion volume is open, while the CI ion volume is closed and with a small hole which allows the exit of the ions. With this latter ion volume, the effective pressure within the ion source is quite high, thus facilitating ion/molecule reactions and hence chemical ionization conditions. The inlet system was modified in order to introduce gases into the ion source through the transfer-line inlet. Gas pressures were regulated with a needle valve and ranged from $\sim 2.0 \times 10^{-6}$ to $\sim 5.0 \times 10^{-5}$ Torr each for diborane and silane, and from $\sim 1.0 \times 10^{-5}$ to $\sim 5.0 \times 10^{-5}$ Torr for helium. These values correspond to the pressures read by a Granville-Phillips (Boulder, CO, USA) ion gauge. Because of the high-pressure conditions employed, ion/molecule reactions readily occur even at the lowest pressure limit. Therefore, all the spectra reported must be in principle considered as CI spectra. However, the EI/CI notation is adopted throughout the paper to distinguish among spectra recorded by using the EI or CI ion volume. Selective ion isolation was performed in order to find out reaction sequences. It was achieved by imposition of the ac isolation waveform voltage applied to the endcap electrodes of the ion trap, in combination with the main rf voltage. After isolation, selected ions were stored for times of about 100 ms in order to allow ion/molecule reactions with neutral species to occur. To this purpose, the software of the instrument was modified to permit variation of storage time of selected ions in the ion trap.

The calculation of the abundances of the single $B_mH_n^{+/-}$ ion species is rather complicated due to the presence of two B isotopes in comparable amounts (10 u, 19.9%; 11 u, 80.1%). Calculation of abundances of the primary ion species of diborane was performed using a deconvolution program named GENANSPE [38]. GENANSPE is a software tool wrote in Visual Basic by colleagues of National Research Council in Padova, Italy, to deconvolute complex inorganic mass spectra even in presence of severe isobaric interferences. The procedure is user-driven and interactive: starting with low mass units, by clicking a peak, several tentative identifications are made by the program by reading the elemental database, combining most common fragments, and calculating a peak cluster with most probable components, every component having a weighting coefficient. By variation of coefficients, every calculated cluster is iteratively compared with the real signal in order to minimize discrepancies.

Collisional-activation (CA) spectra of the most interesting positive product ions were recorded, in order to get information about their connectivity. The ITMS parameters were as following: storage time: 10–20 ms; $q_z$ value: 0.45; helium buffer gas pressure: $6.5 \times 10^{-4}$ Torr; tickle voltage: 4000 mV. In some cases, due to the presence of isobaric ions, double isolations by the apex method were required in order to select and react a

single ion species having the same *m/z* value as other ions. By this procedure, the precursor ion of the charged species under examination is selected in the first step, followed by a suitable reaction time to yield the desired product ion with appreciable abundance, and by the second isolation step. This method is successfully applied only if it is possibile to find a precursor ion yielding just one among isobaric ions.

## 3. Results and discussion

### 3.1. Ion/molecule reactions in diborane

#### 3.1.1. Positive ions

Self-condensation reactions were monitored by storing diborane primary ions $B_2H_n^+$ ($n = 0$–5) for increasing reaction times up to 1 s, at three different gas pressures: $2.0 \times 10^{-7}$, $4.0 \times 10^{-7}$ and $6.0 \times 10^{-7}$ Torr. Primary ions represent by large the most abundant ion family at every reaction time: their total abundance decreases to about 70% of the total ion current (TIC) after 1 s reaction time at $p_{B_2H_6} = 6.0 \times 10^{-7}$ Torr. At the same diborane pressure, boron hydride ion clusters are formed containing up to six B atoms (five B atoms at the lowest pressures): $B_3H_n^+$ ($n = 3$–6), $B_4H_n^+$ ($n = 3$–5), $B_5H_n^+$ ($n = 5$–7) and $B_6H_6^+$. The $B_3H_n^+$ and $B_5H_n^+$ ion clusters are the most abundant among product ion families; the abundance of the $B_3H_n^+$ family decreases when that of $B_5H_n^+$ starts to rise, thus suggesting that the latter originates from the former through condensation followed by dehydrogenation processes. Subsequently, ion/molecule reactions of selected ions were studied and rate constants were determined. The procedure for *k* determination is not straightforward because of peak overlapping among different ions due to the presence of the B isotopes. The $B_2H_n^+$ peak cluster, ranging from $m/z = 20$ to 27, was deconvoluted by the GENANSPE program, yielding the following composition: $B_2^+$, 1.1%; $B_2H^+$, 1.8%; $B_2H_2^+$, 27%; $B_2H_3^+$, 16%; $B_2H_4^+$, 7.4%; $B_2H_5^+$, 47%, in the mass spectrum recorded at 0 ms reaction time and $p_{B_2H_6} = 6.0 \times 10^{-7}$ Torr. However, it does not significantly change after 40 ms, the highest time at which reaction rate constants were determined. Starting from these data, and considering the B isotopes abundances, the contribution of each ion species to every mass peak in the *m/z* 22–27 range was calculated (peaks at *m/z* 20 and 21 are too little abundant to be considered): results are listed in Table 1, and may be considered reliable in the 0–40 ms reaction time range. The very abundant peak at $m/z = 27$ can only correspond to the $^{11}B^{11}BH_5^+$ ion; it was easily selected and stored, but no products were detected. Considering the $m/z = 26$ peak, and knowing that $B_2H_5^+$ is unreactive under the present experimental conditions, selection of this signal allows to identify the ions formed by $B_2H_4^+$ (see Table 1), but it was also found to be unreactive. By iterating this procedure, and by subtracting from each spectrum of isolated ions the contributions of isobar parent and product ions determined from the previous peak, qualitative and quantitative data on the reactivity of diborane primary ions were determined. The same method was applied to the $B_3H_n^+$ and $B_4H_n^+$ ions; here, the task was easier as few ions proved to be reactive. Moreover, the $B_5H_n^+$ and $B_6H_6^+$ ions did not display any reactivity. Rate constants of the reactions observed are reported in Table 2.

Condensation followed by double dehydrogenation is by far the most frequent reaction pathway; the $B_3H_n^+$ and $B_4H_4^+$ ions exclusively react through this path, yielding the corresponding

Table 1
Peak composition of diborane positive mass spectra in the *m/z* 22–27 range, $p_{B_2H_6} = 6.0 \times 10^{-7}$ Torr

| *m/z* | Ion (percentage abundance) | | |
|---|---|---|---|
| 22 | $^{11}B^{11}B^+$ (30%) | $^{10}B^{11}BH^+$ (24%) | $^{10}B^{10}BH_2^+$ (46%) |
| 23 | $^{11}B^{11}BH^+$ (11%) | $^{10}B^{11}BH_2^+$ (83%) | $^{10}B^{10}BH_3^+$ (6.0%) |
| 24 | $^{11}B^{11}BH_2^+$ (76%) | $^{10}B^{11}BH_3^+$ (23%) | $^{10}B^{10}BH_4^+$ (1.0%) |
| 25 | $^{11}B^{11}BH_3^+$ (71%) | $^{10}B^{11}BH_4^+$ (16%) | $^{10}B^{10}BH_5^+$ (13%) |
| 26 | $^{11}B^{11}BH_4^+$ (24%) | $^{10}B^{11}BH_5^+$ (76%) | |
| 27 | $^{11}B^{11}BH_5^+$ (100%) | | |

Table 2
Positive ion/molecule reactions in diborane/nitrogen mixture[a]

| Reaction | $k_{exp}$ | $\Sigma k_{exp}$ | $k_{cap}$[b] | Efficiency[c] | $\Delta H$[d] |
|---|---|---|---|---|---|
| $B_2H^+ + B_2H_6 \rightarrow B_2H_5^+ + B_2H_2$(1) | 4.9 | | | | |
| $B_2H^+ + B_2H_6 \rightarrow B_3H_4^+ + BH_3$(2) | 5.3 | | | | |
| $B_2H^+ + B_2H_6 \rightarrow B_4H_3^+ + 2H_2$(3) | 3.3 | 14 | 15.00 | 0.90 | |
| $B_2H_2^+ + B_2H_6 \rightarrow B_2H_5^+ + B_2H_3$(4) | 1.7 | | | | |
| $B_2H_2^+ + B_2H_6 \rightarrow B_3H_5^+ + BH_3$(5) | 2.2 | | | | −35 |
| $B_2H_2^+ + B_2H_6 \rightarrow B_4H_4^+ + 2H_2$(6) | 1.4 | 5.3 | 14.80 | 0.35 | −13 |
| $B_2H_3^+ + B_2H_6 \rightarrow B_3H_6^+ + BH_3$(7) | 2.5 | | | | |
| $B_2H_3^+ + B_2H_6 \rightarrow B_4H_5^+ + 2H_2$(8) | 1.5 | 4.0 | 14.70 | 0.30 | |
| $B_3H_3^+ + B_2H_6 \rightarrow B_5H_5^+ + 2H_2$(9) | 1.3 | 1.3 | 12.80 | 0.16 | |
| $B_3H_4^+ + B_2H_6 \rightarrow B_5H_6^+ + 2H_2$(10) | 0.40 | 0.40 | 12.75 | 0.030 | |
| $B_3H_5^+ + B_2H_6 \rightarrow B_5H_7^+ + 2H_2$(11) | 0.40 | 0.40 | 12.66 | 0.030 | −1.6 |
| $B_4H_4^+ + B_2H_6 \rightarrow B_6H_6^+ + 2H_2$(12) | 0.80 | 0.80 | 12.03 | 0.070 | −3.9 |
| $N_2^+ + B_2H_6 \rightarrow B_2H_6^+ + N_2$(13) | 3.1 | 3.1 | 14.13 | 0.22 | −97 |

[a] Rate constants are expressed as $10^{-10}$ cm$^3$ molecule$^{-1}$ s$^{-1}$; uncertainty is within 20%.
[b] Collisional rate constants have been calculated according to the parametrized trajectory theory [39] taking the polarizability of diborane from Ref. [40].
[c] Efficiency has been calculated as the ratio $\Sigma k_{exp}/k_{cap}$.
[d] Reaction enthalpies are expressed as kcal mol$^{-1}$ and have been calculated taking heats of formation of $N_2^+$, $N_2$, $BH_3$ and $B_2H_6$ from Ref. [41], of $B_2H_2^+$ from Ref. [42], and of $B_3H_5^+$, $B_4H_4^+$, $B_5H_7^+$ and $B_6H_6^+$ from Ref. [43].

Table 3
Relative abundances of negative ions in diborane

| EI ion volume | | | CI ion volume | | |
|---|---|---|---|---|---|
| $m/z$[a] | Ion | Percentage abundance | $m/z$[a] | Ion | Percentage abundance |
| 24–26 | $B_2H_4^-$ | 5.5 | 37–40 | $B_3H_7^-$ | 8.50 |
| 34–37 | $B_3H_4^-$ | 5.0 | 48–52 | $B_4H_8^-$ | 50.6 |
| 36–39 | $B_3H_6^-$ | 4.6 | 49–53 | $B_4H_9^-$ | 2.3 |
| 37–40 | $B_3H_7^-$ | 29.3 | 57–62 | $B_5H_7^-$ | 6.3 |
| 38–41 | $B_3H_8^-$ | 2.5 | 61–66 | $B_5H_{11}^-$ | 2.3 |
| 46–50 | $B_4H_6^-$ | 2.4 | 68–74 | $B_6H_8^-$ | 3.3 |
| 47–51 | $B_4H_7^-$ | 4.6 | 77–84 | $B_7H_7^-$ | 2.2 |
| 48–52 | $B_4H_8^-$ | 19.9 | 81–88 | $B_7H_{11}^-$ | 2.1 |
| 49–53 | $B_4H_9^-$ | 7.7 | 83–90 | $B_7H_{13}^-$ | 2.3 |
| 58–63 | $B_5H_8^-$ | 2.4 | | | |
| 60–65 | $B_5H_{10}^-$ | 3.3 | | | |

[a] Mass-to-charge ratios calculated by considering the B isotopes.

$B_{n+2}H_{n+2}^+$ ions. Primary ions show a more varied reactivity: besides double dehydrogenation, hydride tranfer leading to $B_2H_5^+$ and $BH_3$ loss are also observed. These results generally agree with the reactions observed by Dunbar in ICR experiments [14]. In his work, Dunbar reported as being exothermic all the double dehydrogenation reactions, while all the pathways leading to $BH_3$ loss were endothermic. Reactions of $B_2H^+$ were not reported by Dunbar, and hydride transfer reactions were not observed. According to Dunbar's results, reactions (5) and (7) in Table 2 are endothermic; however, on the basis of thermochemical data available, reaction (5) is strongly exothermic, while we have found no data on $B_3H_6^+$ in reaction (7). Moreover, almost every reaction of $B_2H_4^+$ and $B_2H_5^+$ is reported by Dunbar to be endothermic; the fact that we did not observe any reaction from these two precursors supports the assumption that in our ITMS experiments ions are formed in their ground electronic state and, therefore, only exothermic reactions are observed.

### 3.1.2. Negative ions

Figs. 1 and 2 show the mass spectra of negative ions of diborane recorded by employing the EI and the CI ion volumes, respectively. Fig. 1 clearly indicates that, even in the electron ionization conditions, ion/molecule reactions take place to a considerable extent (the main peaks in the spectrum are attributable to $B_3H_n^-$ and $B_4H_n^-$ species), due to the high sample pressure employed. When the CI ion volume is used (Fig. 2), condensation reactions occur to a higher degree, and ion clusters of higher mass are observed. Table 3 reports the results of spectra deconvolution of EI and CI experiments; only ions with an abundance higher than 2% of TIC are reported. This time, almost no agreement is found among Dunbar's results and ours, as only $B_4H_9^-$, one of the most abundant ion species detected by Dunbar, is present in Table 3. As sample pressures in our experiments and in the reference are comparable, the only explanation for this discrepancy lies in the different ionization energy, which is much lower than 35 eV in Dunbar's experiments (8 eV). Dunbar identified only one reaction pathway, starting from the $BH_4^-$ ion and not observed here. As far as our experiments are concerned, every attempt to select a single ion species failed, as the signal-to-noise ratio was always too low, and therefore no reaction sequence was determined.

## 3.2. Silane/diborane mixtures

### 3.2.1. Positive ions

Ionization and reaction up to 1 s of $SiH_4/B_2H_6$ mixtures led to formation of mainly two families of mixed ions, containing both Si and B: $SiBH_n^+$ ($n = 2$–4) and $SiB_2H_n^+$ ($n = 1$–5). This results from deconvolution of spectra recorded at the same partial pressure of the reactant gases, i.e., $6.0 \times 10^{-7}$ Torr. Further experiments were carried out at three different partial pressure ratios between the reagents (1:1, 1:3, and 3:1) and at total reactant gas pressure of $1.2 \times 10^{-6}$ Torr, but the overall abundance of mixed ions is almost not affected by relative sample concentrations. At the 1:1 and 1:3 $SiH_4/B_2H_6$ partial pressure ratios, the total mixed ions abundance is slightly higher than in excess of silane (6% versus 5%, approximatively), thus suggesting a minor prevailing role of ions from diborane in the formation of mixed ions.

Table 4 reports the main ion/molecule reactions observed, together with experimental and collisional rate constants, and reaction efficiencies. Self-condensation reactions are not reported as already present in Table 2 (diborane) and Ref. [30] (silane). Reactions of diborane primary ions, $B_2H_n^+$ ($n = 1$–5), were determined by the same procedure adopted in self-condensation of $B_2H_6$. However, the abundances of products of $B_2H^+$ were so low that no rate constants could be determined. $B_3H_n^+$, $B_4H_n^+$ and mixed ions are little abundant; therefore, their isolation produces mass spectra with low-intensity signals, from which no reliable quantitative data could be obtained. These three ion families were isolated and it was found that $B_3H_n^+$ ($n = 3$–6) and $B_4H_n^+$ ($n = 2$–5) yield the $SiB_3H_{n+2}^+$ and $SiB_4H_{n+2}^+$ ions, respectively, while the $SiB_2H_n^+$ ($n = 1$–5) ion species react with silane to form $Si_2B_2H_{n+2}^+$. On the other hand, mass overlapping occurred for $Si^+$ ($m/z = 28$) and $SiH^+$ ($m/z = 29$) silane primary ions, respectively with the $N_2^+$ and $N_2H^+$ ions coming from nitrogen mixed to diborane. When ion species at $m/z = 28$ were selected and stored, two products were detected: (i) a cluster of peaks in the 23–27 $m/z$ range, whose

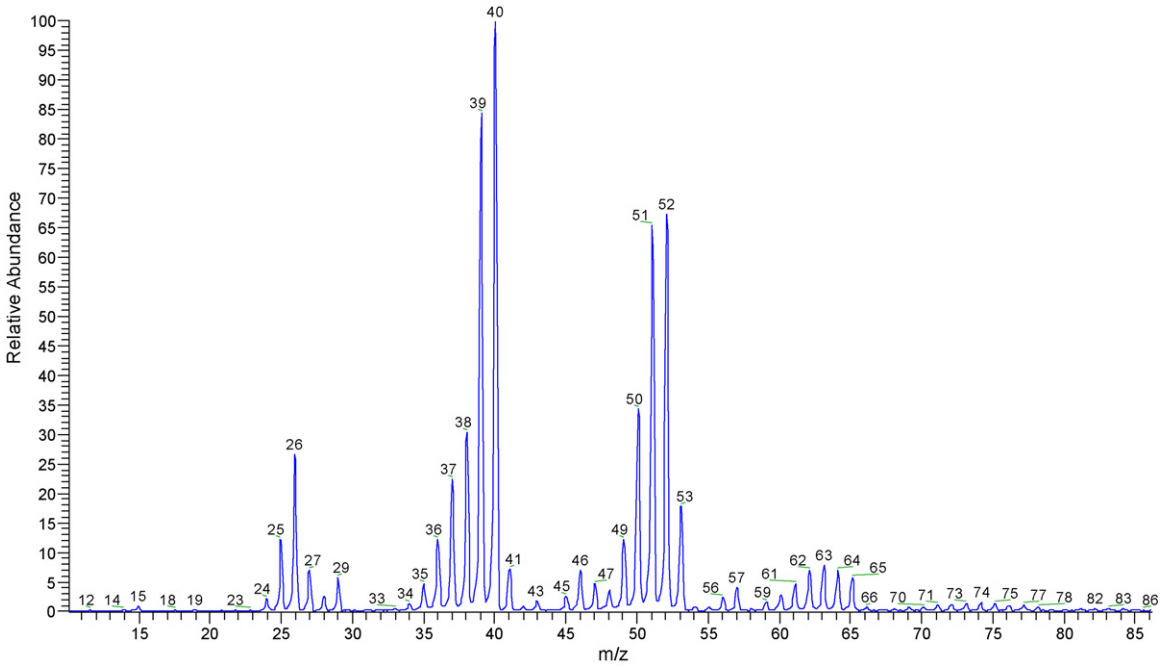


Fig. 1. Mass spectrum of diborane in negative ionization, EI ion volume.

abundances match the isotope distribution of two boron atoms, thus indicating the formation of ionized diborane and its following fragmentation to the $B_2H_n^+$ ($n = 1$–5) ions; (ii) a product ion at $m/z = 31$. The $N_2^+$ ion reacts with $B_2H_6$ by charge-exchange, as observed in the nitrogen/diborane mixture previously studied (Table 2), and as predicted by the ionization energies of $N_2$ and $B_2H_6$ [41]. Moreover, Si displays a lower ionization energy than $B_2H_6$ [41]; therefore, it may be assumed that charge-exchange only occurs starting from the $N_2^+$ ion. For the product at $m/z = 31$, we may assume that it is the product of charge-exchange between $N_2^+$ and $SiH_4$, on the basis of the relative ionization energies of nitrogen and silane [41]; due to this chemical ionization, $SiH_4^+$ loses one hydrogen atom yielding the observed $SiH_3^+$ ion.

Selection of ions at $m/z = 29$ yields the product $SiH_3^+$ ($m/z = 31$); moreover, weak signals attributable to the $B_2H_5^+$ ($m/z = 25$–27) ions appear in the spectra after about 20 ms reaction time. Since the $N_2H^+$ ion was found to be unreactive in the

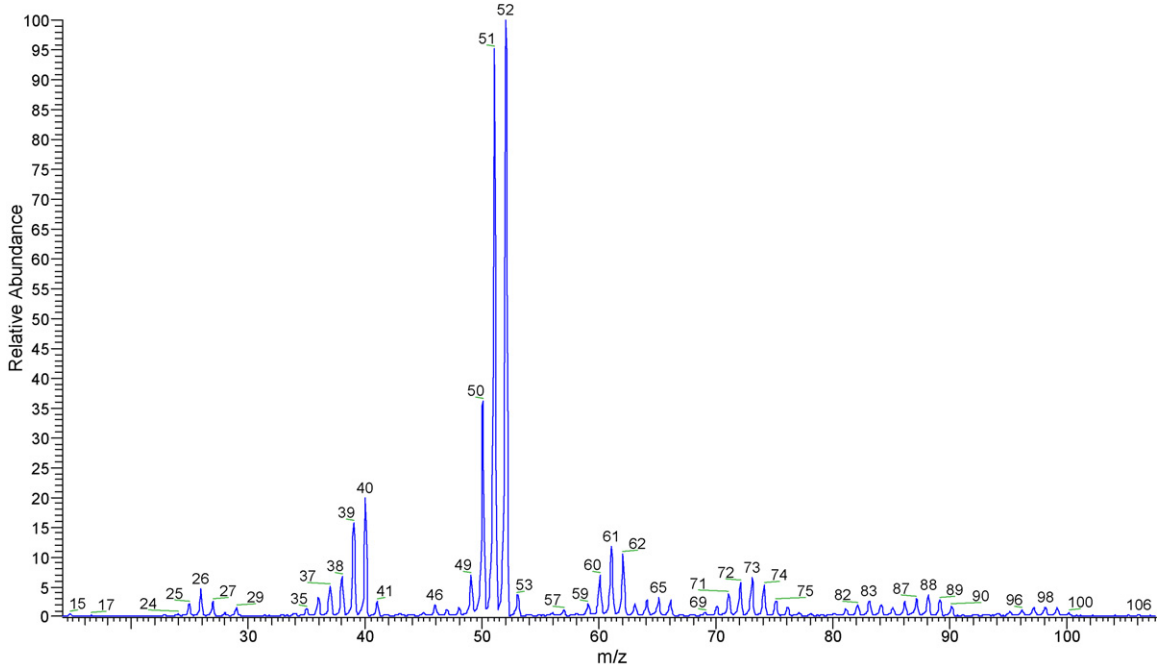


Fig. 2. Mass spectrum of diborane in negative ionization, CI ion volume.

Table 4
Positive ion/molecule reactions in silane/diborane mixtures[a]

| Reaction | $k_{exp}$ | $\Sigma k_{exp}$ | $k_{cap}$[b] | Efficiency[c] | $\Delta H$[d] |
|---|---|---|---|---|---|
| Diborane primary ions | | | | | |
| $B_2H_2^+ + SiH_4 \rightarrow SiBH_3^+ + BH_3$ | 5.0 | | | | ≤308 |
| $B_2H_2^+ + SiH_4 \rightarrow SiB_2H_2^+ + 2H_2$ | 1.2 | | | | ≤332 |
| $B_2H_2^+ + SiH_4 \rightarrow SiB_2H_4^+ + H_2$ | 5.3 | 11.5 | 13.14 | 0.88 | ≤332 |
| $B_2H_3^+ + SiH_4 \rightarrow SiBH_4^+ + BH_3$ | 2.0 | | | | ≤249 |
| $B_2H_3^+ + SiH_4 \rightarrow SiB_2H_5^+ + H_2$ | 1.7 | 3.7 | 12.99 | 0.28 | ≤273 |
| $B_2H_4^+ + SiH_4 \rightarrow B_2H_5^+ + SiH_3$ | 1.7 | 1.7 | 12.85 | 0.13 | −1.5 |
| Silane primary ions | | | | | |
| $SiH_2^+ + B_2H_6 \rightarrow B_2H_5^+ + SiH_3$ | 11 | 11 | 13.89 | 0.79 | −5.1 |
| $SiH_3^+ + B_2H_6 \rightarrow B_2H_5^+ + SiH_4$ | 9.5 | 9.5 | 13.78 | 0.69 | −6.6 |
| Silane secondary ions | | | | | |
| $Si_2H_3^+ + B_2H_6 \rightarrow Si_2B_2H_7^+ + H_2$ | 1.1 | 1.1 | 12.13 | 0.09 | |

[a] Rate constants are expressed as $10^{-10}$ cm$^3$ molecule$^{-1}$ s$^{-1}$; uncertainty is within 20%.
[b] Collisional rate constants have been calculated according to the Parametrized Trajectory Theory [39] taking the polarizability of silane and diborane from Ref. [40].
[c] Eficiency has been calculated as the ratio $\Sigma k_{exp}/k_{cap}$.
[d] Reaction enthalpies are expressed as kcal mol$^{-1}$ and have been calculated taking heats of formation of $SiH_3$, $SiH_4$, $SiH_2^+$, $SiH_3^+$, $BH_3$ and $B_2H_6$ from Ref. [41], and of $B_2H_n^+$ ($n$ = 2–4) from Ref. [42]. When silicon–boron ions are formed, $\Delta H$ are referred as the upper limits of the heats of formation (kcal mol$^{-1}$) of product ions.

diborane/nitrogen mixture, formation of $SiH_3^+$ is ascribed to the following reaction:

$$SiH^+ + B_2H_6 \rightarrow SiH_3^+ + B_2H_4 \quad (14)$$

On the other hand, $B_2H_5^+$ is formed by $SiH_3^+$ reacting with diborane, as confirmed by isolation and storage of $SiH_3^+$ (Table 2). In addition, product ions in the 42–43 and 53–55 $m/z$ ranges are observed, and are ascribed to the reactions:

$$SiH^+ + B_2H_6 \longrightarrow SiBH_4^+ + BH_3 \quad \text{m/z 42,43} \quad (15)$$

$$SiH^+ + B_2H_6 \longrightarrow SiB_2H_5^+ + H_2 \quad \text{m/z 53-55} \quad (16)$$

The CA spectrum of the $SiBH_4^+$ ion (Fig. 3) features a peak at $m/z$ = 29, which corresponds to $SiH^+$. This suggests a $HSi^+$–$BH_3$ connectivity for the parent $SiBH_4^+$ ion. On the other hand, collisional activation of $SiB_2H_5^+$ only yields loss of $H_2$, and this neutral loss was again observed when the $SiB_2H_3^+$ daughter ion was in turn isolated. Finally, the low signal intensity prevented from CA of $SiB_2H^+$, and no information about connectivity could be gained.

Primary ions of both species display an overall good reactivity. When silane is the neutral reagent, condensation followed by dehydrogenation is the most frequent path observed. However, loss of $BH_3$ also occurs quite frequently, and it is interesting to note that this neutral formation, which was often observed in self-condensation of diborane, takes place even when the neutral reagent is not $B_2H_6$, thus suggesting $BH_3$ formation as a very favourable exit channel. On the other hand, when $B_2H_6$ is the neutral reagent, $BH_3$ or $H_2$ losses are seldom observed. Instead, hydride transfer is the most frequent path, as it occurs for every silane primary ion reacting with $B_2H_6$. As a consequence, mixed ions are preferably formed in reactions of diborane ions with silane. The $SiBH_3^+$ ion was selected by double isolation starting from the $B_2H_2^+$ precursor ion. CA spectrum of $SiBH_3^+$ shows a peak at $m/z$ 41 and one at $m/z$ 28 (Fig. 4), this latter corresponding to $Si^+$. This suggests an ion structure similar to that of $SiBH_4^+$, with the $BH_3$ moiety connected to silicon. Double isolation of $SiB_2H_2^+$ and $SiB_2H_4^+$ from the same precursor $B_2H_2^+$ was performed and the CA spectra were recorded; however, as in the case of $SiB_2H_5^+$, only $H_2$ loss was observed.

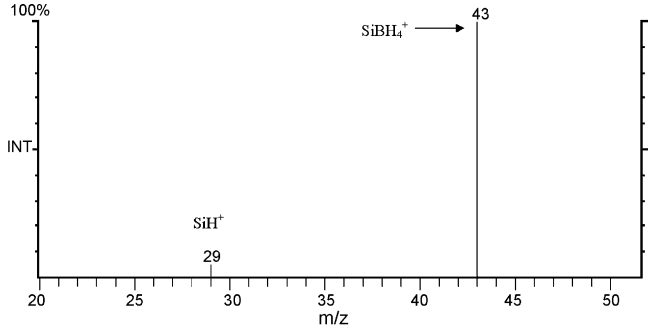


Fig. 3. Collisional activation spectrum of mass-selected $SiBH_4^+$.

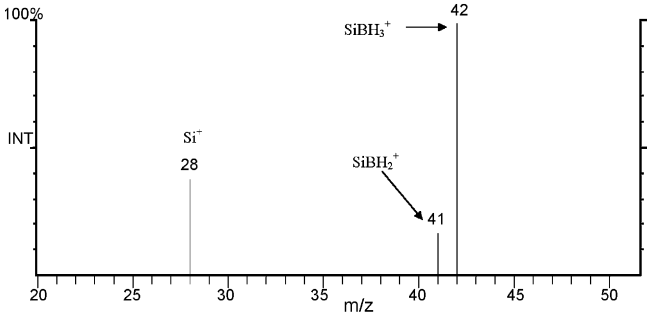


Fig. 4. Collisional activation spectrum of mass-selected $SiBH_3^+$.

Table 5
Negative ion/molecule reactions in silane/diborane mixtures

$SiH_3^- + B_2H_6 \rightarrow SiBH_6^- + BH_3$
$Si_2H^- + B_2H_6 \rightarrow Si_2BH_4^- + BH_3$
$Si_2H^- + B_2H_6 \rightarrow Si_2B_2H_5^- + H_2$
$Si_2H_2^- + B_2H_6 \rightarrow Si_2BH_5^- + BH_3$
$Si_2H_2^- + B_2H_6 \rightarrow Si_2B_2H_6^- + H_2$
$Si_2H_3^- + B_2H_6 \rightarrow Si_2BH_6^- + BH_3$
$Si_2H_3^- + B_2H_6 \rightarrow Si_2B_2H_7^- + H_2$
$Si_2H_4^- + B_2H_6 \rightarrow Si_2BH_7^- + BH_3$
$Si_2H_5^- + B_2H_6 \rightarrow Si_2BH_8^- + BH_3$
$Si_3^- + B_2H_6 \rightarrow Si_3BH_3^- + BH_3$
$Si_3H^- + B_2H_6 \rightarrow Si_3BH_4^- + BH_3$
$Si_3H^- + B_2H_6 \rightarrow Si_3B_2H_5^- + H_2$
$Si_3H_2^- + B_2H_6 \rightarrow Si_3BH_5^- + BH_3$
$Si_3H_2^- + B_2H_6 \rightarrow Si_3B_2H_6^- + H_2$
$Si_3H_3^- + B_2H_6 \rightarrow Si_3BH_6^- + BH_3$
$Si_3H_3^- + B_2H_6 \rightarrow Si_3B_2H_7^- + H_2$
$Si_4H^- + B_2H_6 \rightarrow Si_4BH_4^- + BH_3$
$Si_4H_2^- + B_2H_6 \rightarrow Si_4BH_5^- + BH_3$
$Si_4H_3^- + B_2H_6 \rightarrow Si_4BH_6^- + BH_3$

Table 6
Negative ion abundances in silane/diborane, CI ion volume[a]

| *m/z*[b] | Ion | Percentage abundance |
|---|---|---|
| 44, 45 | $SiBH_6^-$ | 3.8 |
| 56 | $Si_2^-$ | 4.7 |
| 57 | $Si_2H^-$ | 8.6 |
| 70, 71 | $Si_2BH_4^-$ | 2.0 |
| 81–83 | $Si_2B_2H_5^-$ | 6.1 |
| 84 | $Si_3^-$ | 6.9 |
| 85 | $Si_3H^-$ | 7.5 |
| 86 | $Si_3H_2^-$ | 2.3 |
| 87 | $Si_3H_3^-$ | 2.4 |
| 97, 98 | $Si_3BH_3^-$ | 3.2 |
| 112 | $Si_4^-$ | 10.6 |
| 113 | $Si_4H^-$ | 8.0 |
| 140 | $Si_5^-$ | 7.6 |
| 141 | $Si_5H^-$ | 5.7 |

[a] The percentage abundances of the ions are calculated with respect to the total ion current (TIC), which also includes ions whose abundance does not reach 2%. These latter ions are not reported in the table.
[b] Mass-to-charge ratios calculated by considering the B isotopes.

When thermochemical data were available, all the reactions resulted to be exothermic. On the assumption of the exothermicity of the reactions observed, upper limits for the heats of formation of mixed Si–B ions were estimated. Results are reported in Table 4.

### 3.2.2. Negative ions

In a first experiment, diborane was introduced into the ion source, while leaking silane in the ion trap. In this way, ions from diborane were formed and stored in the trap in the presence of silane. However, even at ion storage times up to 1 s, no reactions were observed. In the subsequent experiment, silane was ionized and diborane was leaked in the ion trap. This time, a considerable number of product ions was observed. It is noticeable that a certain amount of sample gas introduced in the ion source leaks into the ion trap: this is evidenced by the fact that ion products of silane self-condensation reactions are present among mixed ions. Moreover, ion/molecule reactions readily occur even in the ion source, expecially when high sample pressures and the CI ion volume are employed. Mass selection of silane ions allowed determination of reaction sequences. As silane self-condensation reactions were already studied in a preceding paper [34], in Table 5 only reactions of silane ions with diborane are reported.

The reactions display a very regular trend. With few exceptions, every reaction follows two parallel paths, leading to condensation followed by $BH_3$ and to $H_2$ loss. In every case, the most abundant ion product comes from $BH_3$ loss. This is the only path displayed by the $Si_4H_n^-$ ($n = 1$–3) ions, likely because dehydrogenation is not favoured for such ions having a low hydrogen content. Ab initio studies of reactions of $B_2H_6$ with $SiH_4$ [13] or $NH_3$ [22] show, in both cases, an initial coordination leading to the M–$BH_3$–$BH_3$ complex (M = $NH_3$, $SiH_4$). If sufficient energy is provided, the neutral complex evolves to $BH_3$ or $H_2$ elimination. In these reactions, $B_2H_6$ acts as a Lewis acid and M as a Lewis base; in particular, Hu et al. [13] indicate $SiH_4$–$BH_3$ as an electron donor–acceptor complex, in which $SiH_4$ acts as electron donor through a partially negative charged hydrogen atom. We may postulate that, in the presence of a stronger nucleophilic species such as a negative ion, the reaction with $B_2H_6$ may occur, through a similar mechanism, at thermal energies as in our experiments, where it is assumed that helium buffer gas pressure is sufficient to thermalize the reactant ions.

Due to the almost total absence in the literature of heats of formation of negative ions considered here, only one upper limit to the heat of formation was calculated, i.e., the one of $SiBH_6^-$ formed from $SiH_3^-$ and $B_2H_6$. This was estimated to be $\leq$47.5 kcal mol$^{-1}$ [41].

Fig. 5 reports the negative mass spectrum obtained by ionizing silane (CI ion volume) and by leaking $B_2H_6$ into the ion trap. Therefore, the signals in the spectrum correspond to ions formed in self-condensation of silane and in reactions of silane ions with diborane. Spectrum devoconvolution by GENANSPE yields the ion abundances, which are reported in Table 6, where only ions whose abundance is higher than 2% of TIC are shown. However, on the overall amount of ions in the spectra, the total concentration of mixed ions is about 22%, which is much higher than the total abundance of positive mixed ions in the same mixture (5%, Section 3.2.1). This can be considered a consequence of the electrophilic character of $B_2H_6$. When it reacts with more nucleophilic species (silane anions in our case), it can act as a Lewis acid, and $BH_3$ and $H_2$ losses are the most favourable reaction paths. This means that one or two B atoms are retained in the ionic product, thus forming a mixed ion. On the other hand, when $B_2H_6$ reacts with silane cations, few mixed ions are formed, as the main product is $B_2H_5^+$. This result resembles a chemical ionization (CI) mass spectrometric study of boron hydrides [44], in which CI of $B_2H_6$ by using $CH_4$ as reagent gas exclusively yields $B_2H_5^+$ as B-containing ion, according to the exothermic reaction:

$$CH_5^+ + B_2H_6 \rightarrow B_2H_5^+ + CH_4 + H_2 \quad (17)$$

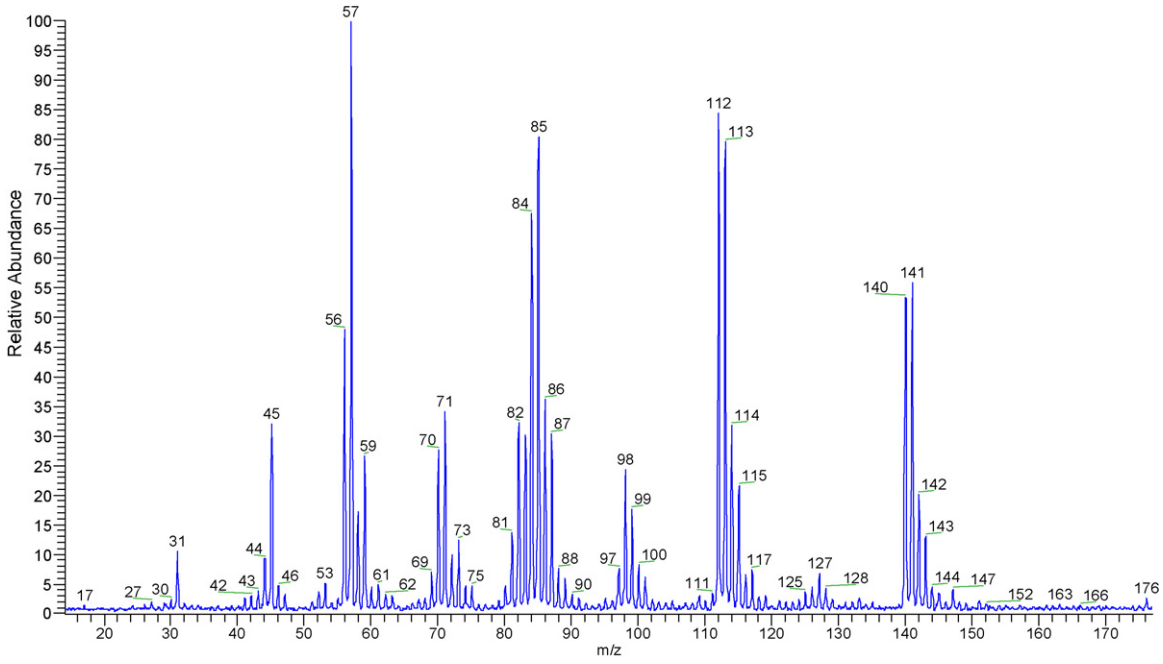


Fig. 5. Mass spectrum of silane/diborane in negative ionization of silane, CI ion volume.

Among diborane cations, only the $B_2H_n^+$ ($n = 1$–3), $B_3H_n^+$ and $B_4H_n^+$ ions react with silane to give mixed ions, and with appreciable efficiencies only for $B_2H_2^+$ and $B_2H_3^+$. On the other hand, diborane anions did not display any reactivity towards silane under the present experimental conditions. In view of these results, it seems that neutral diborane contributes to formation of mixed ions to a much larger extent than its positive or negative ions.

## 4. Conclusions

Positive and negative ion/molecule reactions in silane/diborane mixtures were studied by ion trap mass spectrometry, with the aim of unraveling the ionic processes occurring during PE-CVD of gaseous mixtures containing $SiH_4$ and $B_2H_6$ as volatile sources of Si and B. Positive ions give a small contribution to formation of Si–B bonds, while in negative ionization the Si/B ions abundance is about four times higher. This is ascribed to efficient reactions of $B_2H_6$ with silane anions that follow typical paths of diborane behaving as a Lewis acid. On the other hand, diborane anions were unreactive toward $SiH_4$ in our experiments. In the literature, we have found very few information about boron hydride anions reactivity: besides the work of Dunbar [14], studies of reactions of $B_2H_3^-$ with $CO_2$, $CS_2$ and COS are reported [17,18]. We may conclude that a more acidic neutral species than silane could efficiently react with diborane anions. However, the present results demonstrate that the contribution of negative ions in the plasma-CVD processes is worth of consideration, and that the gas-phase chemistry of anions deserves further attention in view of fundamental and applicative studies.

## Acknowledgements

The authors would like to acknowledge financial supports from the University of Torino and from Italian MIUR through the ‘Cofinanziamento di Programmi di Ricerca di Rilevante Interesse Nazionale’.

## References

[1] R.J. Matyi, D.L. Chapek, D.P. Brunco, S.B. Felch, B.S. Lee, Surf. Coat. Technol. 93 (1997) 247.
[2] S. Inoue, Manufacture of Semiconductor Integrated Circuits, JP 63307724 (1988).
[3] Toshiba Corp. Integrated Circuits. JP 59111324 (1984).
[4] R.E.I. Schropp, K.F. Feenstra, E.C. Molenbroe, H. Meiling, J.K. Rath, Philos. Mag. B76 (1997) 309.
[5] K.L. Chopra, P.D. Paulson, V. Dutta, Prog. Photovolt.: Res. Appl. 12 (2004) 69.
[6] H. Meiling, A.M. Brockhoff, J.K. Rath, R.E.I. Schropp, Mat. Res. Soc. Symp. Proc. 507 (1998) 879.
[7] J.G. Ekerdt, Y.-M. Sun, A. Szabo, G.J. Szulczewski, J.M. White, Chem. Rev. 96 (1996) 1499.
[8] S.M. Gates, Chem. Rev. 96 (1996) 1519.
[9] C. Voz, D. Peirò, J. Bertomeu, D. Soler, M. Fonrodona, J. Andreu, Mater. Sci. Eng. B69–70 (2000) 278.
[10] H. Habuka, S. Akiyama, T. Otsuka, W.-F. Qu, J. Cryst. Growth 209 (2000) 807.
[11] M. Adachi, S. Tsukui, K. Okuyama, J. Nanopart. Res. 5 (2003) 31.
[12] S. Hu, J. Kim, P. Tarakeshwar, K.S. Kim, J. Phys. Chem. A 106 (2002) 6817.
[13] S. Hu, Y. Wang, X.-Y. Wang, J. Phys. Chem. A 107 (2003) 1635.
[14] R.C. Dunbar, J. Am. Chem. Soc. 90 (1968) 5676.
[15] R.C. Dunbar, J. Am. Chem. Soc. 93 (1971) 4167.
[16] R.C. Dunbar, J. Phys. Chem. 76 (1972) 2467.
[17] M. Krempp, R. Damrauer, C.H. DePuy, Y. Keheyan, J. Am. Chem. Soc. 116 (1994) 3629.
[18] Z.-W. Qu, H. Zhu, Z.-S. Li, Q.-Y. Zhang, J. Comput. Chem. 23 (2002) 414.

[19] C.H. DePuy, R. Garayev, J. Hankin, G.E. Davico, M. Krempp, R. Damrauer, J. Am. Chem. Soc. 120 (1998) 5086.
[20] X. Zeng, G.E. Davico, J. Phys. Chem. A 107 (2003) 11565.
[21] L.A. Curtiss, J.A. Pople, J. Chem. Phys. 89 (1988) 4875.
[22] M.L. McKee, J. Phys. Chem. 96 (1992) 5380.
[23] L.D. Betowski, M. Enlow, J. Mol. Struct. (THEOCHEM) 638 (2003) 189.
[24] M.L. Mandich, W.D. Reents Jr., M.F. Jarrold, J. Chem. Phys. 88 (1988) 1703.
[25] M.L. Mandich, W.D. Reents Jr., K.D. Kolenbrander, J. Chem. Phys. 92 (1990) 437.
[26] M.L. Mandich, W.D. Reents Jr., J. Chem. Phys. 95 (1991) 7360.
[27] W.D. Reents Jr., M.L. Mandich, J. Chem. Phys. 96 (1992) 4429.
[28] K. Raghavachari, J. Chem. Phys. 96 (1992) 4440.
[29] K. Raghavachari, J. Chem. Phys. 95 (1991) 7373.
[30] L. Operti, M. Splendore, G.A. Vaglio, A.M. Franklin, J.F.J. Todd, Int. J. Mass Spectrom. Ion Processes 136 (1994) 25.
[31] C. Pak, J.C. Rienstra-Kiracofe, H.F. Schaefer III, J. Phys. Chem. A 104 (2000) 11232.
[32] W.G. Xu, J.C. Yang, W.S. Xiao, J. Phys. Chem. A 108 (2004) 11345.
[33] W.D. Reents Jr., J. Am. Soc. Mass Spectrom. 10 (1999) 918.
[34] L. Operti, R. Rabezzana, G.A. Vaglio, Rapid Commun. Mass Spectrom. 20 (2006) 2696.
[35] L. Operti, R. Rabezzana, F. Turco, G.A. Vaglio, Int. J. Mass Spectrom. 232 (2004) 139.
[36] L. Operti, R. Rabezzana, F. Turco, G.A. Vaglio, J. Mass Spectrom. 39 (2004) 682.
[37] L. Operti, R. Rabezzana, F. Turco, G.A. Vaglio, J. Mass Spectrom. 39 (2004) 665.
[38] C. Pagura, S. Valcher, Institute for Energetics and Interphases of CNR, C.so Stati Uniti, 4-35127 PADOVA – Italy – GENANSPE – a software tool for spectra intepretation and de-convolution – Internal Report 1998–2004. A copy of the program can be asked by e-mail to c.pagura@ieni.cnr.it.
[39] T. Su, W.J. Chesnavich, J. Chem. Phys. 76 (1982) 5183.
[40] E.R. Lippincot, J.M. Stutman, J. Phys. Chem. 68 (1964) 2926.
[41] S.G. Lias, J.E. Bartmess, J.F. Liebman, J.L. Holmes, R.D. Levin, W.G. Mallard, J. Phys. Chem. Ref. Data 17 (Suppl. 1) (1988).
[42] M.J.S. Dewar, M.L. McKee, J. Am. Chem. Soc. 99 (1977) 5231.
[43] T.P. Fehlner, W.S. Koski, J. Am. Chem. Soc. 86 (1964) 581.
[44] J.J. Solomon, R.F. Porter, J. Am. Chem. Soc. 94 (1972) 1443.